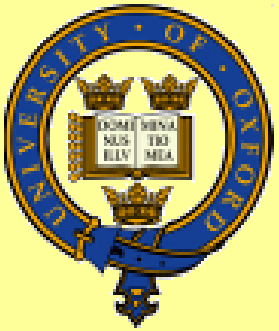

Univerza v Ljubljani
Fakulteta za matematiko in fiziko

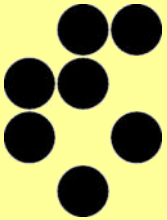

Liquid Crystal Colloids: Functionalization of Inclusions and Continuum

M. Ravnik[1,2], I. Musevic[3,2], J. M. Yeomans[1], S. Zumer[2,3]

[1] University of Oxford, Oxford, UK
[2] University of Ljubljana, Ljubljana, SI
[3] Josef Stefan Institute, Ljubljana, SI

Support of the EC under the Marie Curie project ACTOIDS is acknowledged. The contents reflect only the author's views and not the views of the EC.

Outline

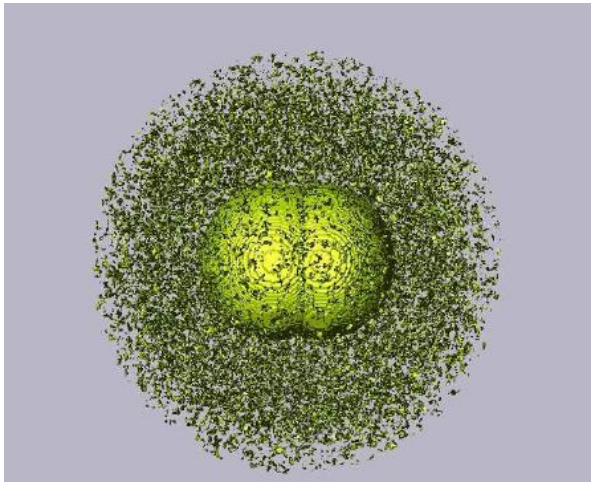

@ introduction

@ theory and modeling

@ functionalization of inclusions: role of shape, Janus surface anchoring profile, topological charge, surface structure

@ functionalization of continuum: material activity and confinement

@ conclusion

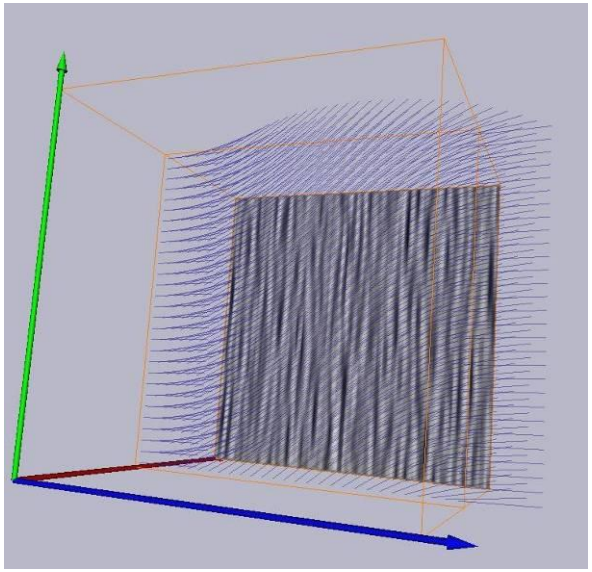

Introduction - Colloids:Assembly

Various types of materials and (self)assembly:

Droplets:Phase separation

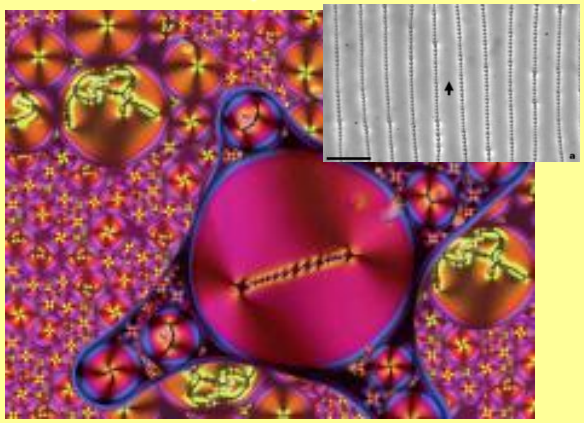

P. Poulin, et al, Science 275, 1770 (1997)
J.-C. Loudet, et al, Nature 407, 611(2000)

Droplets:Surface trapping

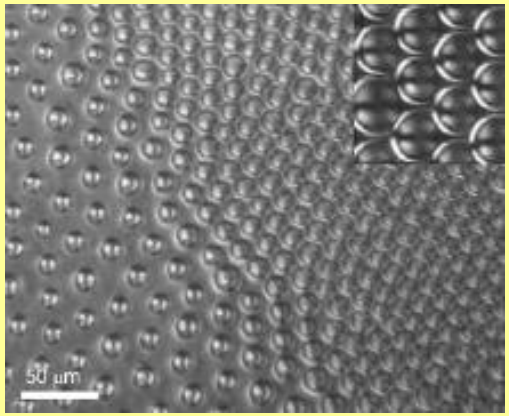

A. B. Nych, et al, PRL 98, 057801(2007)

Solid beads:Optical tweezers

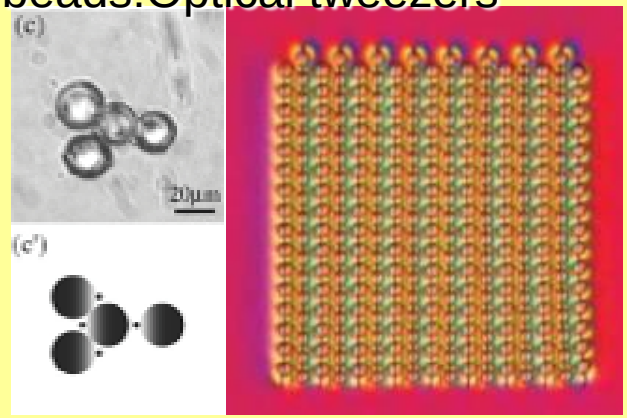

M. Yada, et al, PRL 92, 185501(2004)
I. Musevic, et al, Science 313, 954 (2006)

Solid beads:Electrophoresis

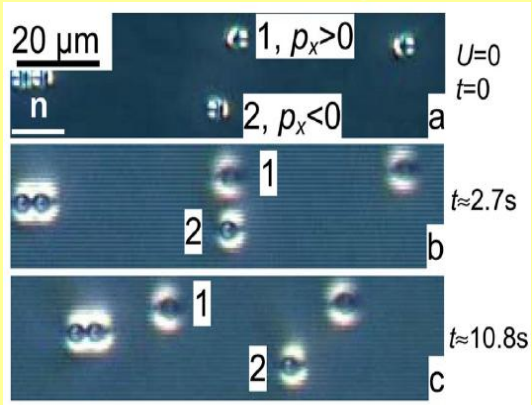

O. P. Pishnyak, et al, PRL 99, 127802 (2007)

Introduction - Nematodynamics & Activity

Materials have internal motility (e.g. swarms of bacteria):

- Nematodynamics

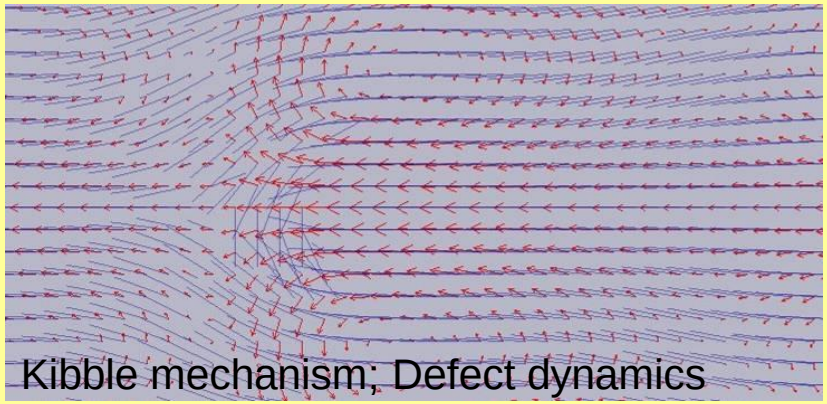

Kibble mechanism; Defect dynamics

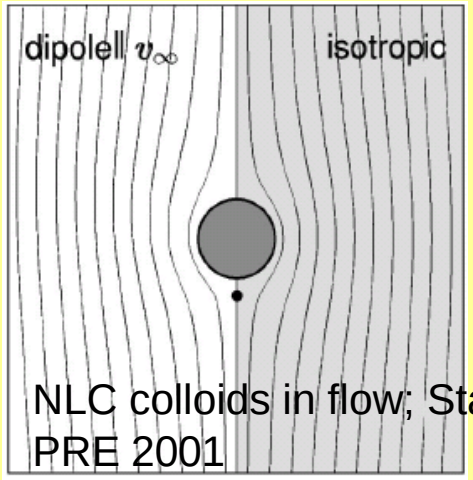

NLC colloids in flow; Stark et al PRE 2001

- Active nematodynamics

Design flow states

Bio-patterns

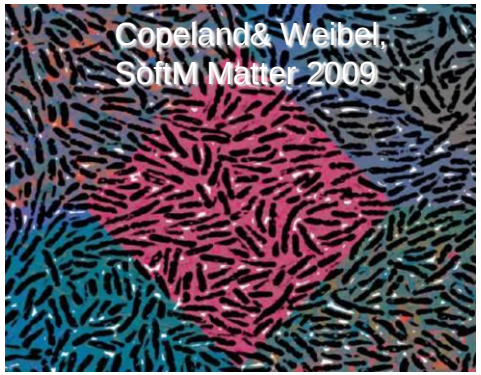

Copeland& Weibel, SoftM Matter 2009

Dombrowski et al, PRL 2004

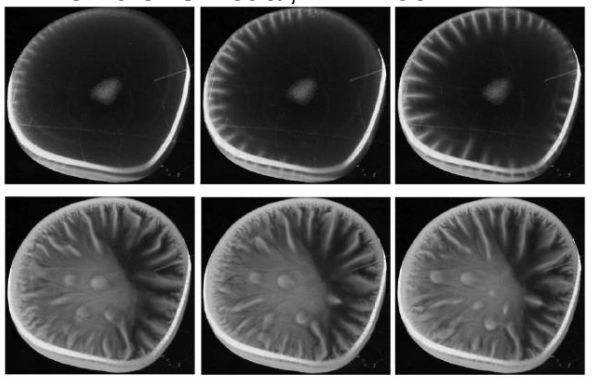

FIG. 1. Bioconvection in a sessile drop of diameter 1 cm. Top: images 5 min apart show the traveling-wave bio-Boycott convection that appears first at the drop edge. Bottom: images 2 min apart show self-concentration seen from above, beginning as vertical plumes which migrate outward.

Dreyfus et al, Nature 2005

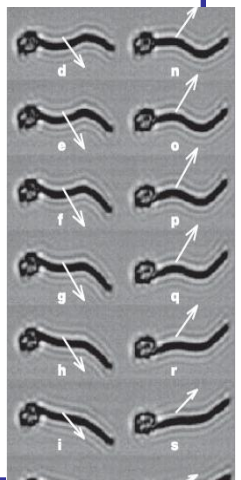

Theory + Modelling

Order parameter tensor:

$$Q_{ij} = \frac{S}{2}(3n_i n_j - \delta_{ij}) + \frac{P}{2}(e_i^{(1)} e_j^{(1)} - e_i^{(2)} e_j^{(2)})$$

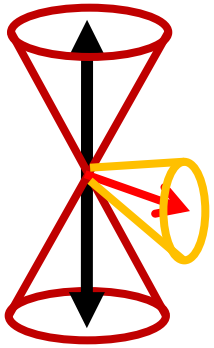

5 degrees of freedom: director, degree of order, secondary director, biaxallity

I. Equilibrium physics of static NLC

$$F = + \frac{1}{2}L\int_{LC}\left(\frac{\partial Q_{ij}}{\partial x_k}\right)\left(\frac{\partial Q_{ij}}{\partial x_k}\right)dV \quad \leftarrow \textit{elasticity}$$

$$+ \int_{LC}\left(\frac{1}{2}AQ_{ij}Q_{ji} + \frac{1}{3}BQ_{ij}Q_{jk}Q_{ki} + \frac{1}{4}C(Q_{ij}Q_{ji})^2\right)dV \quad \leftarrow \textit{order}$$

$$+ \frac{1}{2}W\int_{Surf.Col.}(Q_{ij} - Q_{ij}^0)(Q_{ji} - Q_{ji}^0)dS \quad . \quad \leftarrow \textit{surface}$$

Landau – de Gennes phenomenological free energy

Numerical relaxation on cubic mesh:

Euler-Lagrange equations

$$\frac{d}{dx_k}\frac{\partial F}{\partial \frac{\partial Q_{ij}}{\partial x_k}} - \frac{\partial F}{\partial Q_{ij}} = u_{ij}^{(bulk)} = 0$$

$$\frac{\partial F}{\partial \frac{\partial Q_{ij}}{\partial x_k}} \cdot \nu_k = u_{ij}^{surf.} = 0$$

→ relaxation algortihm $\gamma\frac{dQ_{ij}}{dt} = u_{ij}$ → equil. order. paramet. tenzor profile

Ravnik & Zumer, Liq. Cryst. (2009)

Theory + Modelling

II. Nematodynamics + Activity

Hybrid Lattice Boltzman algorithm: finite differences for Q dynamics and LB for Navier-Stokes flow dynamics.

molecular field

$$(\partial_t + \vec{u}\cdot\nabla)\mathbf{Q} - \mathbf{S}(\mathbf{W},\mathbf{Q}) = \Gamma\mathbf{H} + \lambda\Delta\mu\mathbf{Q}$$

Material derivative

LC alignment in flow (tumbling/aligning)

activity

$$\rho(\partial_t + u_\beta\partial_\beta)u_\alpha$$

$$= \partial_\beta(\Pi_{\alpha\beta}) + \eta\partial_\beta(\partial_\alpha u_\beta + \partial_\beta u_\alpha + (1 - 3\partial_\rho P_0)\partial_\gamma u_\gamma\delta_{\alpha\beta})$$

Stress tensor

viscosity

possible compressibility

LB scheme:

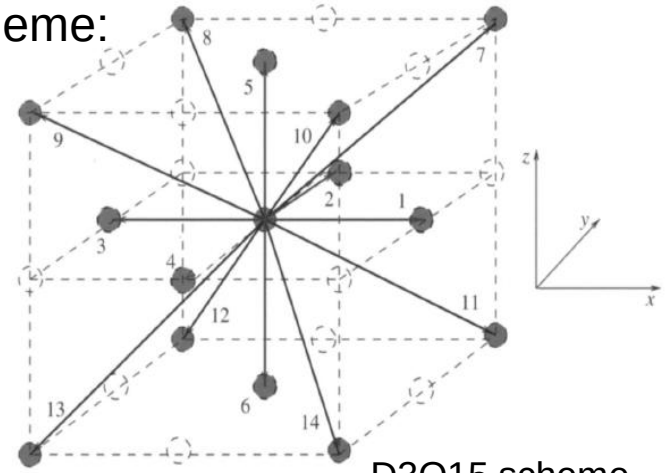

D3Q15 scheme

Distribution functions f_i:

$$\rho = \sum_i f_i, \qquad \rho u_\alpha = \sum_i f_i e_{i\alpha},$$

Streaming and collision:

$$f_i(\boldsymbol{x} + \boldsymbol{e}_i\Delta t, t + \Delta t) - f_i(\boldsymbol{x}, t) = \tfrac{1}{2}\Delta t[\mathcal{C}_{fi}(\boldsymbol{x}, t, \{f_i\}) + \mathcal{C}_{fi}(\boldsymbol{x} + \boldsymbol{e}_i\Delta t, t + \Delta t, \{f_i^*\})]$$

$$\mathcal{C}_{fi}(\boldsymbol{x}, t, \{f_i\}) = -\frac{1}{\tau_f}(f_i(\boldsymbol{x}, t) - f_i^{\mathrm{eq}}(\boldsymbol{x}, t, \{f_i\})) + p_i(\boldsymbol{x}, t, \{f_i\})$$

Denniston et al, Phil. Trans 362, 1745 (2004)

Theory + Modelling

Numerical parameters and characteristics:

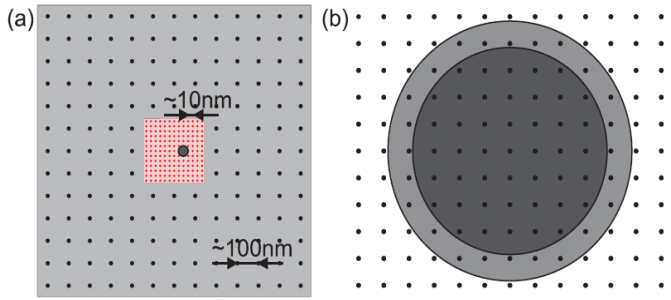

- coupled cubic mesh (10nm and 100nm)
- parallel multi-thread computer code
- typical number of mesh points:
  few 100 x few 100 x few 100 = few 10^7 (max: 600 x 600 x 600 = 2 x 10^8)
- basic parameter values: ξ_N = 6.63nm, S_{bulk}=0.533, strong surf. anchor.

Nematodynamics vs equilibrium static nematic:

- memory requirements increase by ~ 10x

- evaluation time increses by ~10-100x ; (for equal number of evaluation steps)

- crucial coupling of LC and LB time scale (stability)

- activity is effectively introduced by single phenomenological parameter in stress tensor

$$\Pi_{\alpha\beta} = \Pi^{\text{passive}}_{\alpha\beta} + \Pi^{\text{active}}_{\alpha\beta} \qquad \Pi^{\text{active}}_{\alpha\beta} = \zeta \Delta\mu Q_{\alpha\beta}$$

(can be switched-off to yield passive nematodynamics)

$$\Pi^{\text{passive}}_{\alpha\beta} = -P_0\delta_{\alpha\beta} + 2\xi\left(Q_{\alpha\beta} + \frac{1}{3}\delta_{\alpha\beta}\right)Q_{\gamma\varepsilon}H_{\gamma\varepsilon}$$
$$- \xi H_{\alpha\gamma}\left(Q_{\gamma\beta} + \frac{1}{3}\delta_{\gamma\beta}\right) - \xi\left(Q_{\alpha\gamma} + \frac{1}{3}\delta_{\alpha\gamma}\right)H_{\gamma\beta}$$
$$- \partial_\alpha Q_{\gamma\nu}\frac{\delta\mathcal{F}}{\delta\partial_\beta Q_{\gamma\nu}} + Q_{\alpha\gamma}H_{\gamma\beta} - H_{\alpha\gamma}Q_{\gamma\beta}.$$

Particle shape - ellipsoids

Ellipsoidal particels can break symmetry of the director:

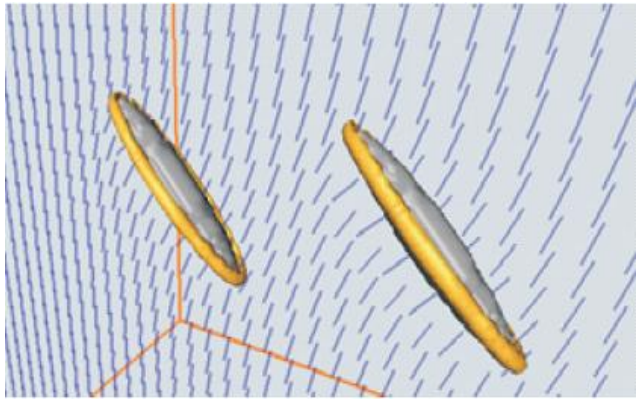

parallel inclination

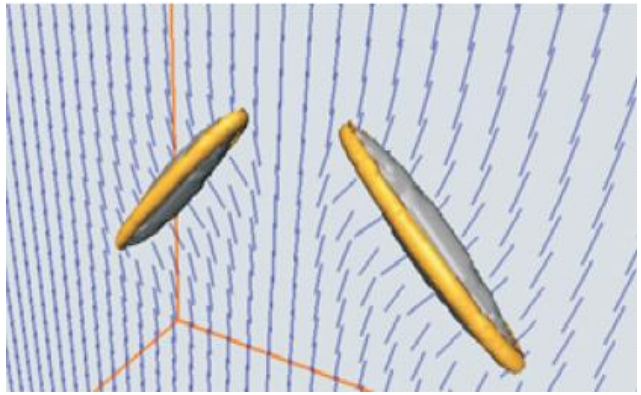

anti-parallel inclination

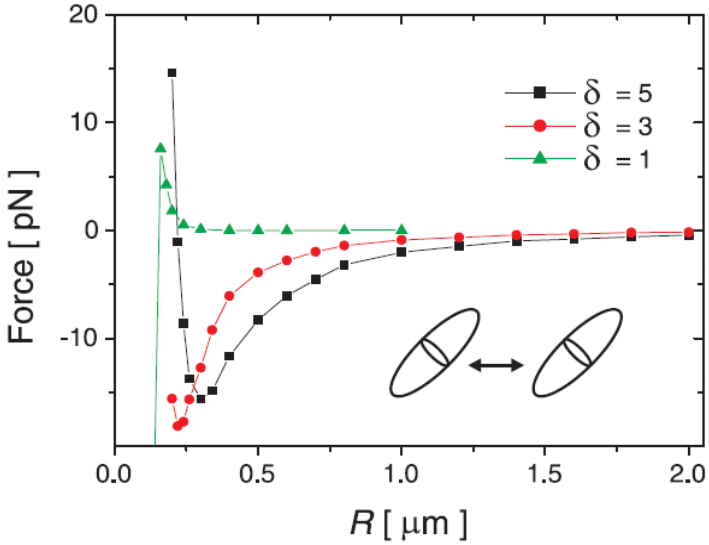

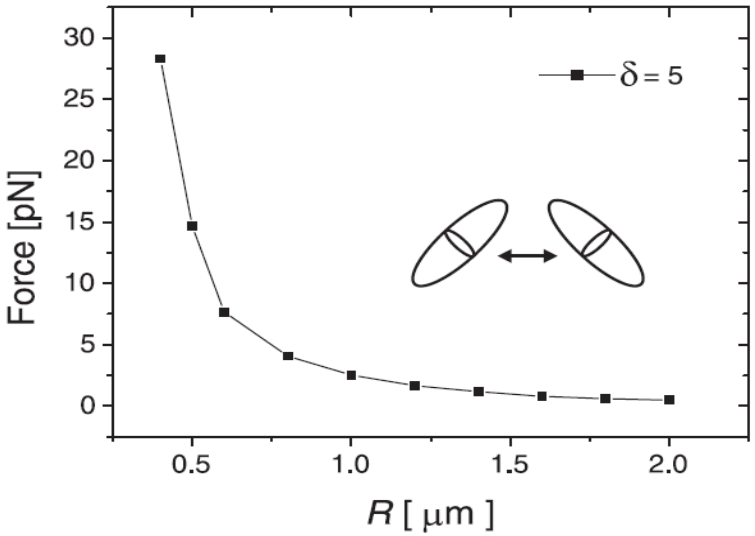

Janus particles

Functionalization of particles by surface anchoring design

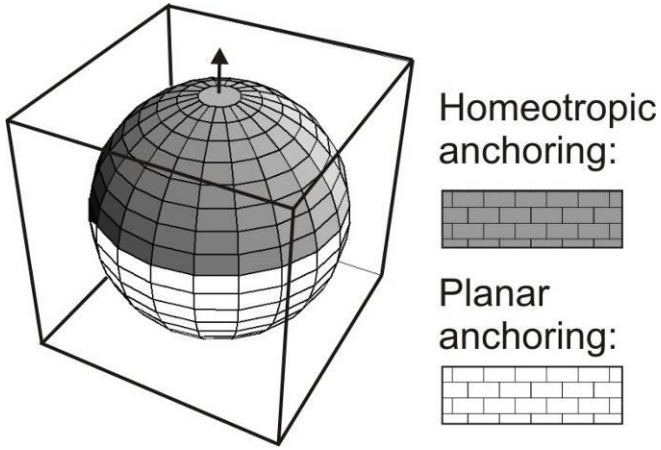

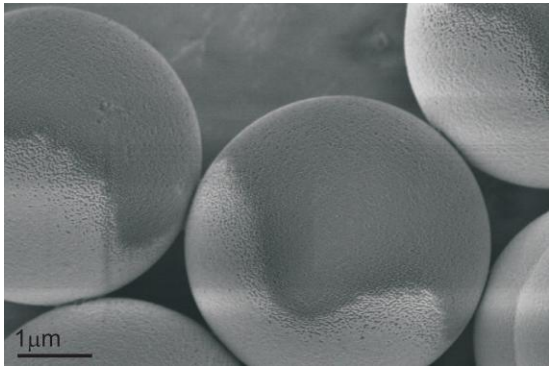

- Gold deposition - planar anchoring
- DMOAP hometropic sufactant

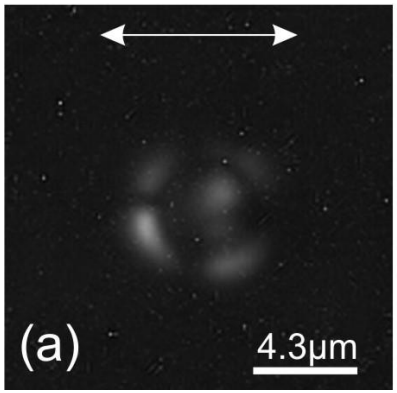

Crossed polars

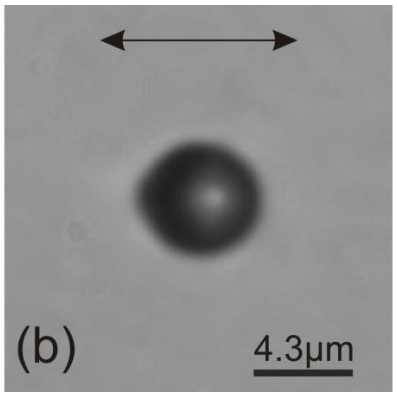

Opt. microsc.

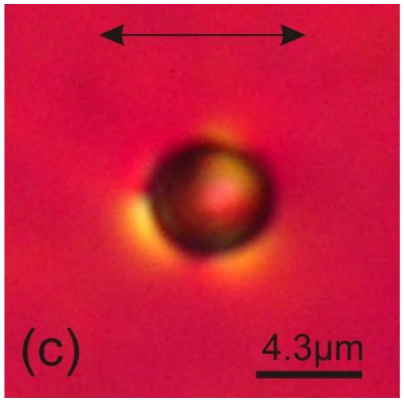

Retardation plate

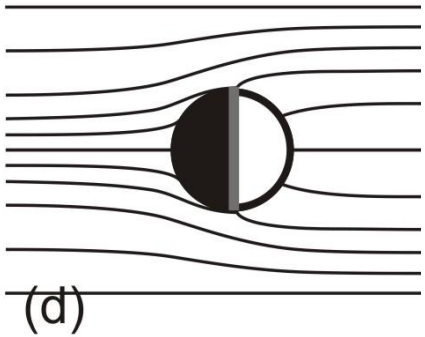

Janus particles

Bistability in (meta)stable particle orientations

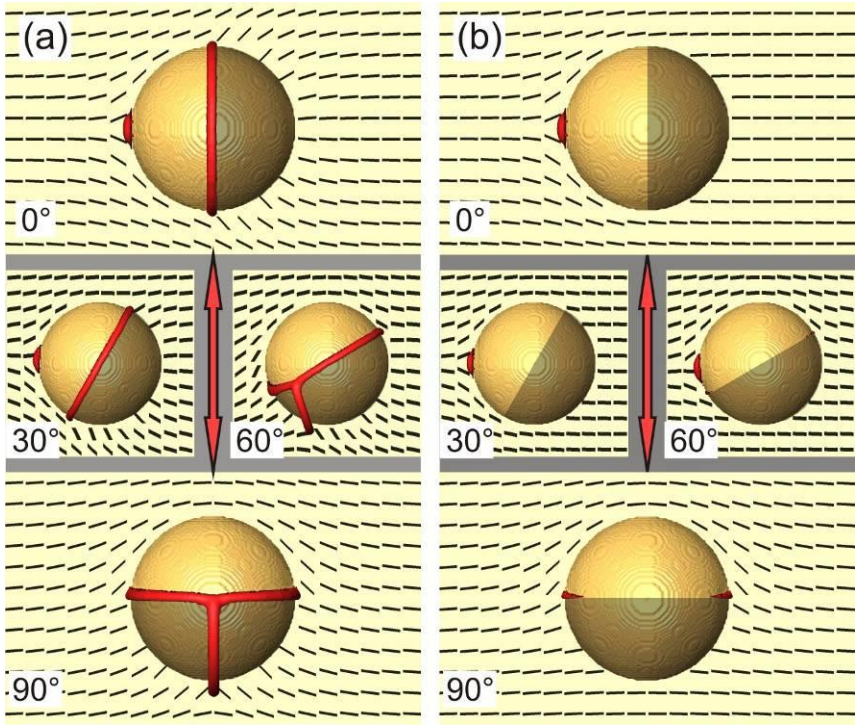

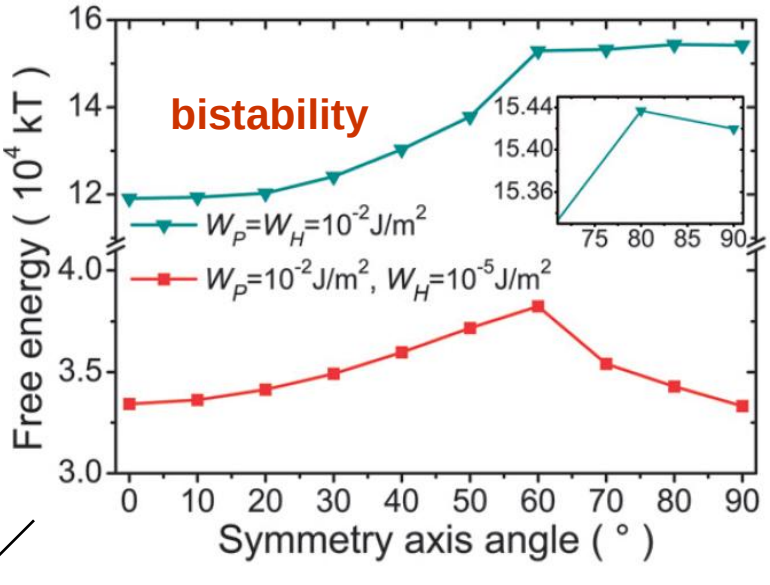

$W_p = W_h = 10^{-2}$ J/m^2 $W_p = 10^{-2}$ J/m^2 $W_h = 10^{-5}$ J/m^2

Energy minima can be tuned by relative surface anchoring strengths.

Possible application: light shutter

“Higher-order” Janus particles

Particles with homeotropic/planar surface patches:

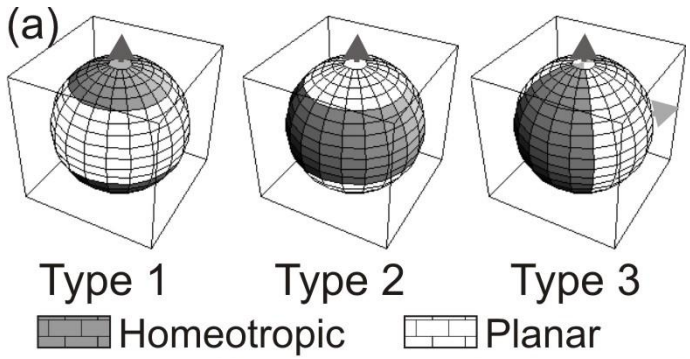

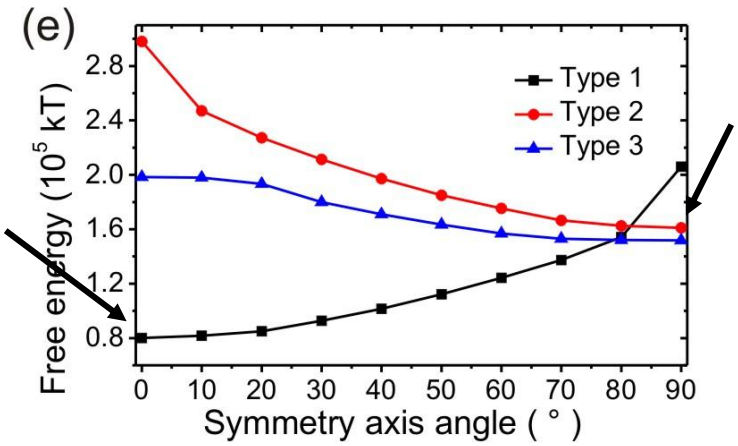

Controllable torques and equilibrium orientation

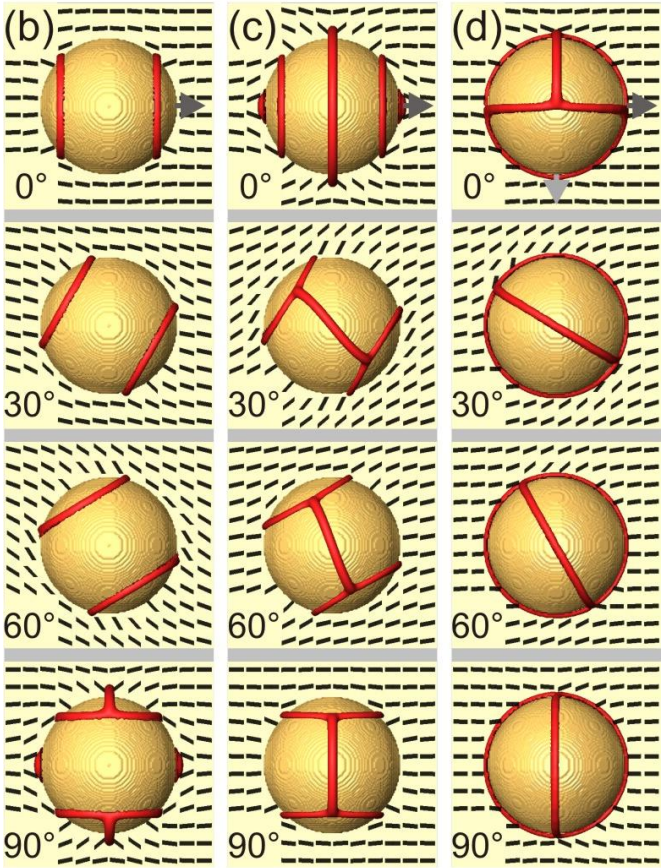

Structure: tiles of director corresponding to relevant surface patches

Topological charge 2 particles

By generalizing topological anchoring profile, spherical particles with higher-than-one topological charge can be designed:

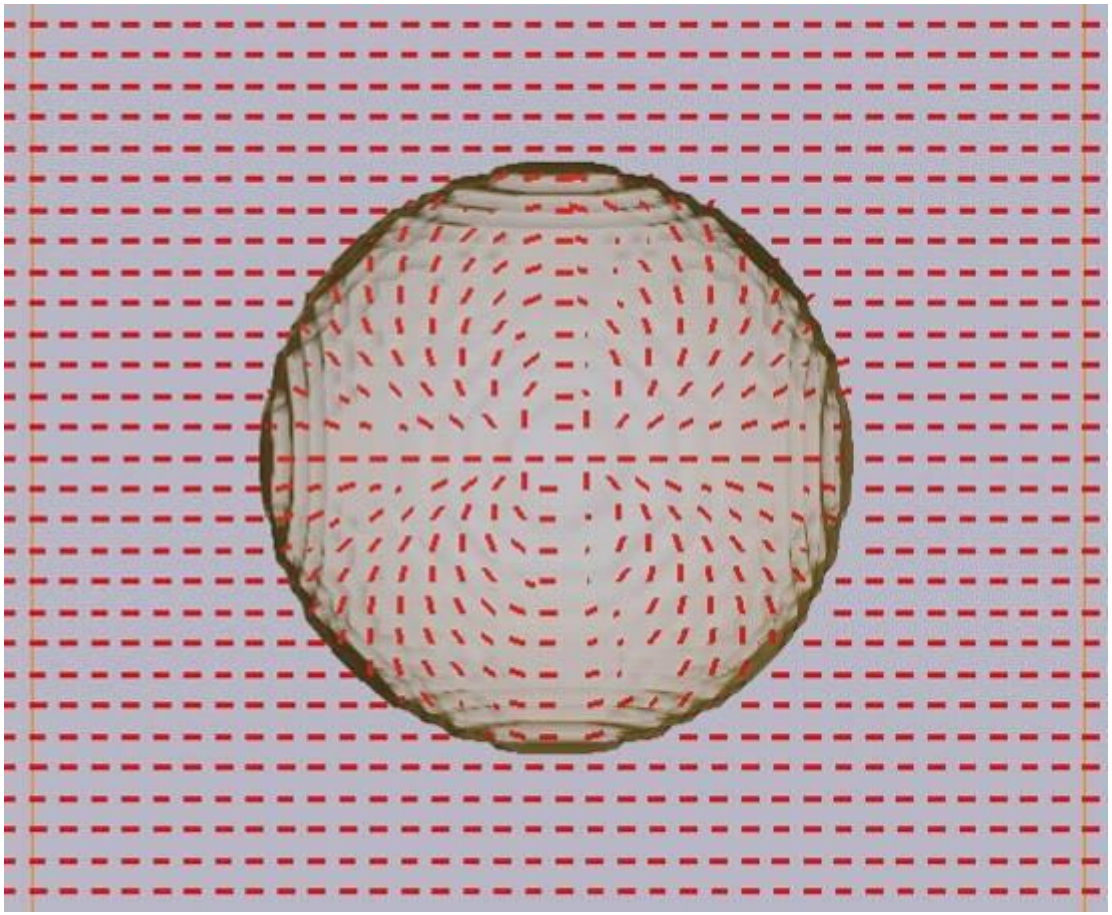

topological charge = 2

Topological charge 2 particles

Two possible compensations:

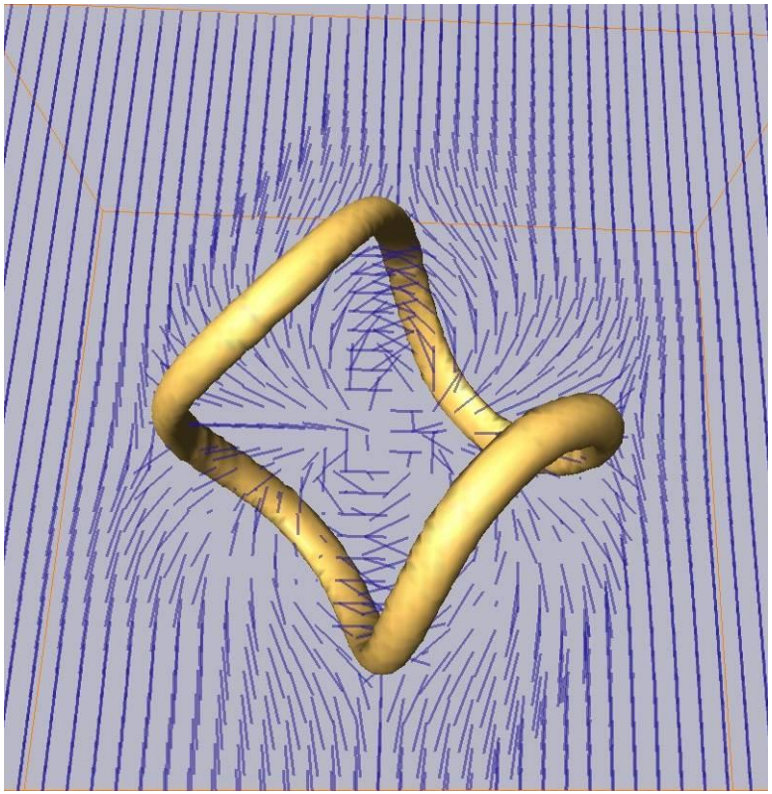

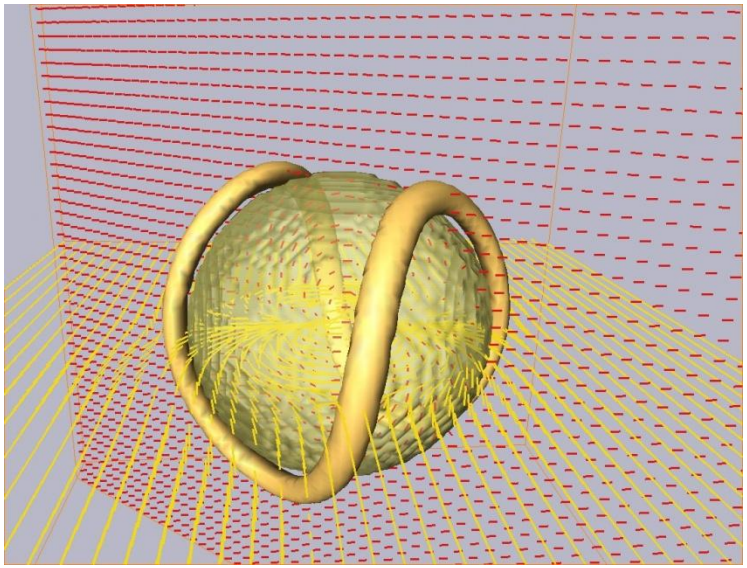

single -1/2 “cage-loop”

Bonus: director is analyticaly given at the particle surface hence it changes can be analytically followed along the full loop.

Tuning interparticle potential

Elastic dipoles and quadrupoles

$$V_{PP}(\mathbf{R}) = \frac{1}{R^3}(1 - 3\cos^3\theta)$$

$$V_{CC}(\mathbf{R}) = \frac{1}{R^5}(9 - 90\cos^2\theta + 105\cos^4\theta)$$

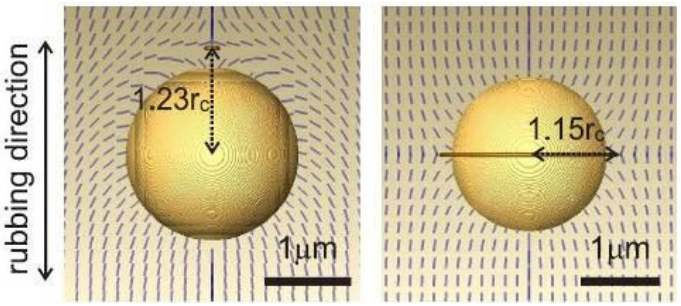

I. Particle shape / director symmetry

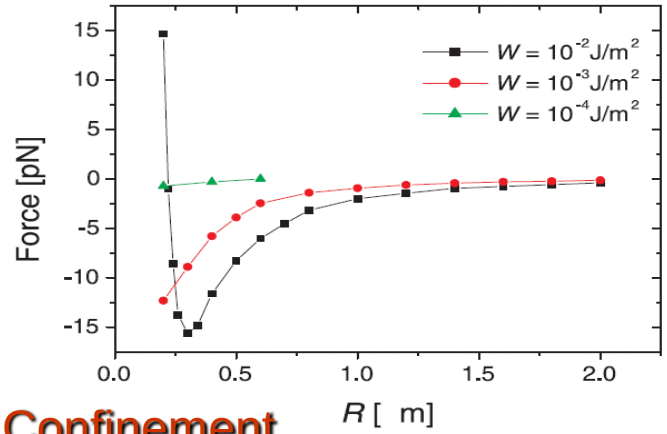

$$\mathcal{F} \propto 1/R^n$$

fit for W = 10^{-2} J/m^2: n = 2.02

fit for W = 10^{-2} J/m^2: n = 2.1

II. Confinement

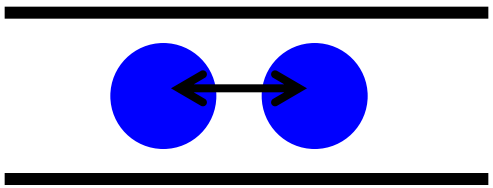

$$\nabla^2 n_\mu = 0$$

$$n_\mu = \sum_n \sin\left(\frac{n\pi}{h}z\right)\left[A_n I_n(\frac{n\pi}{h}\rho) + B_n K_n(\frac{n\pi}{h}\rho)\right]$$

$$K_n(x) = \sqrt{\frac{\pi}{2x}}e^{-x}$$

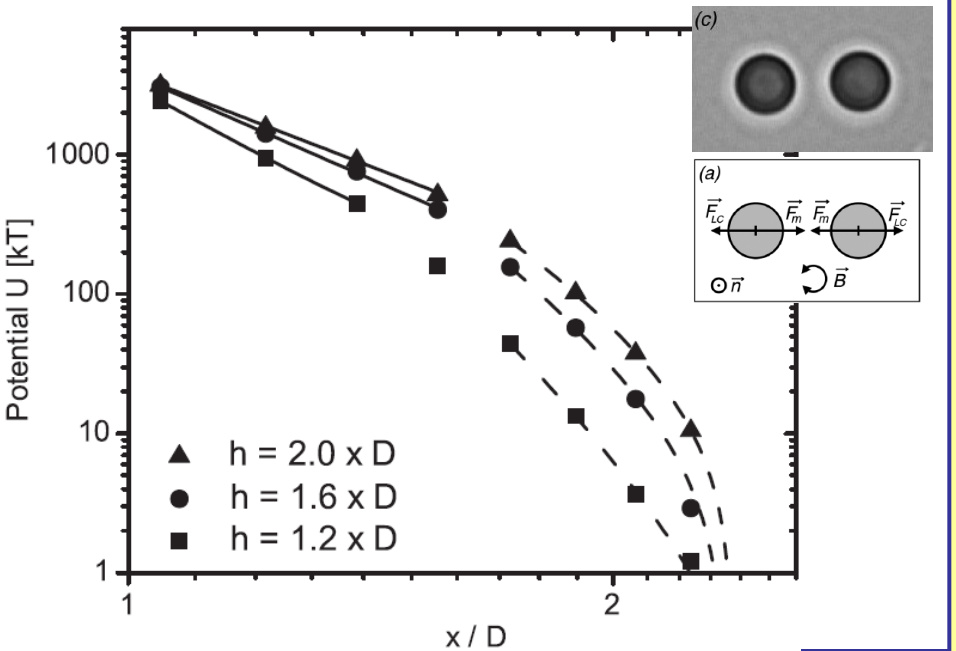

Active flow in confined cell

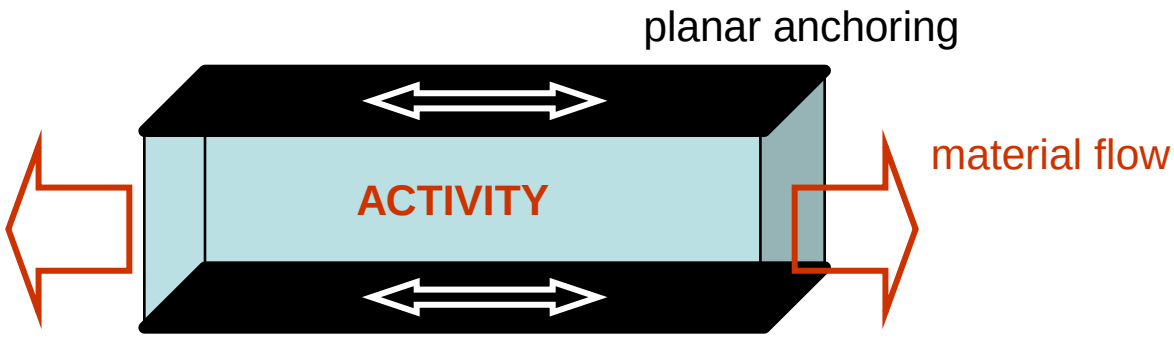

Active flow profiles in planar nematic cell with thickness of 2 μm. 2D in-plane flow profiles:

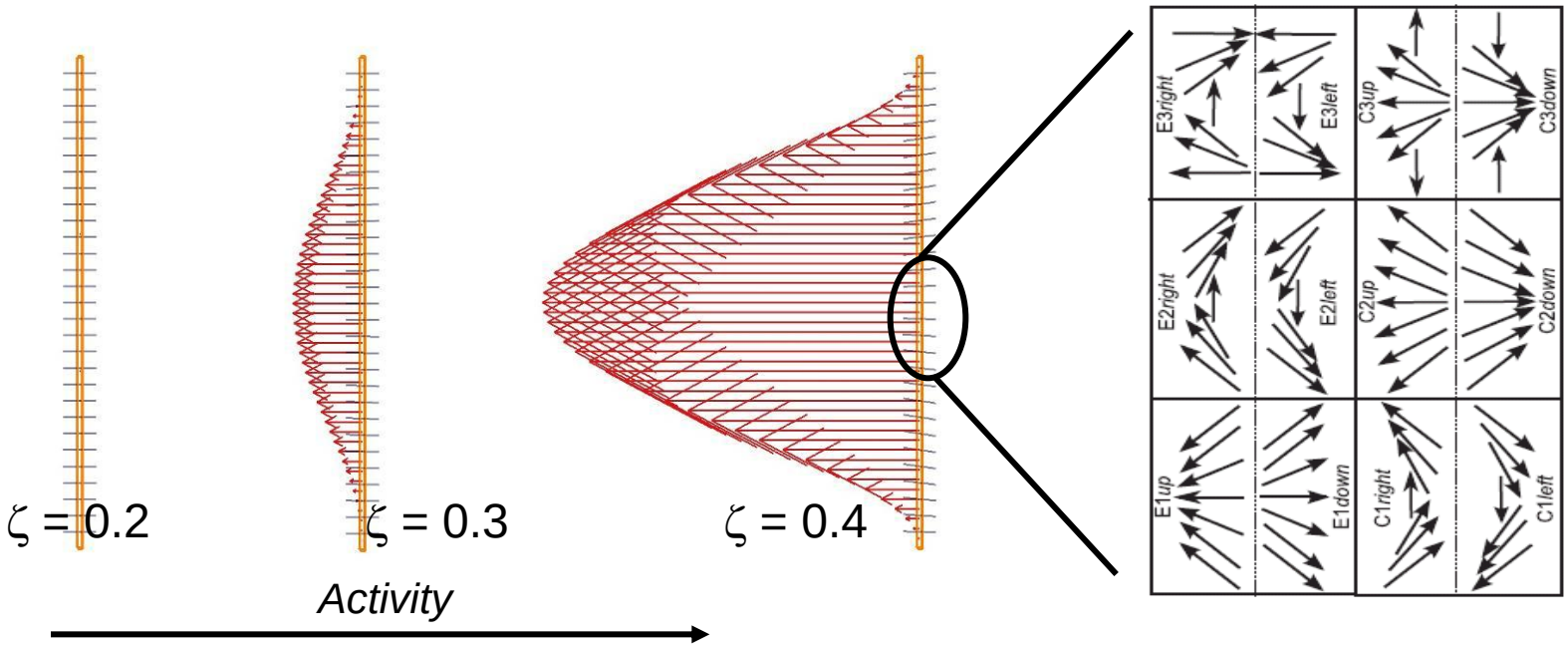

Active flow in confined cell

3D flow profiles are found.

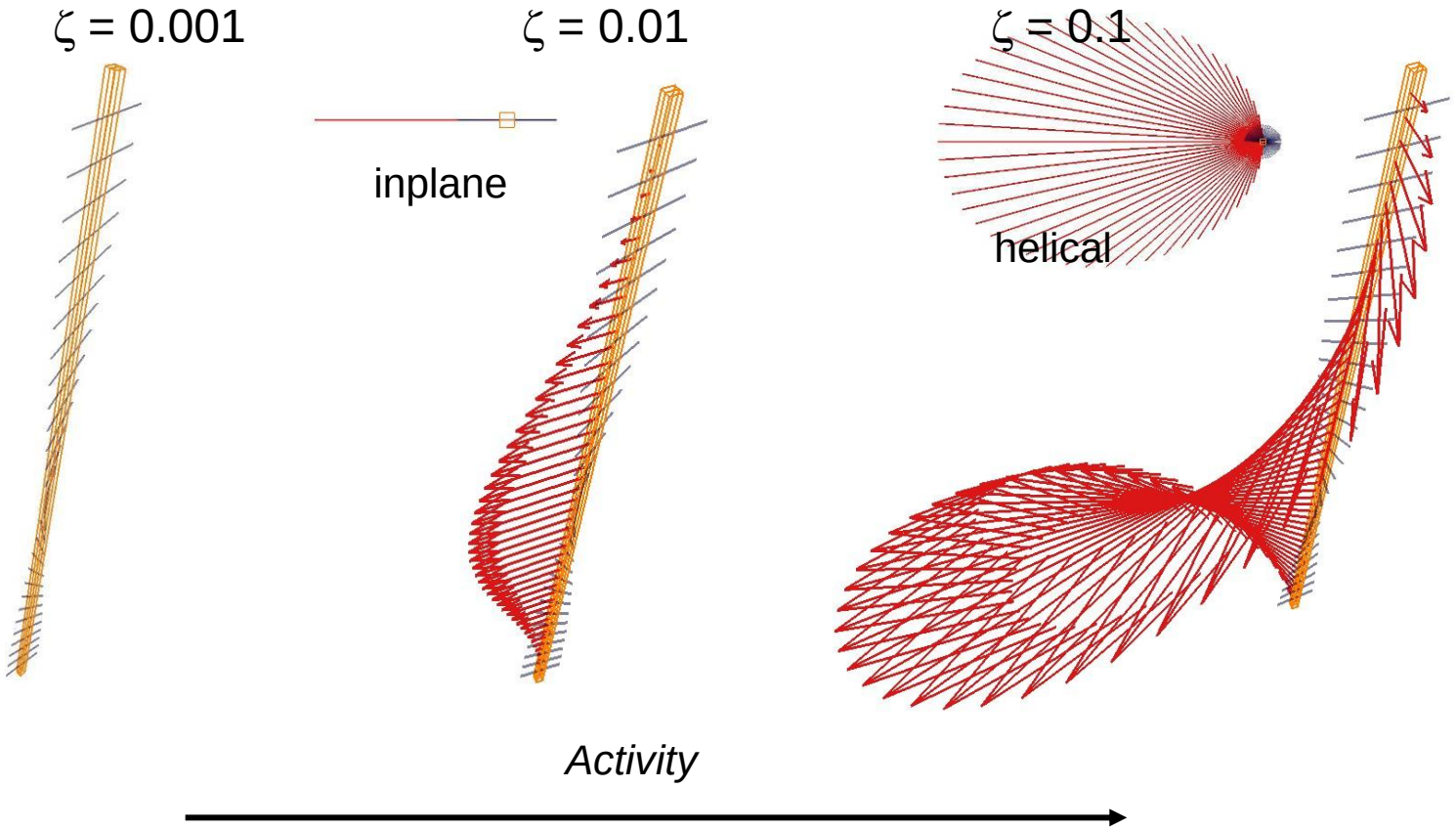

Flow can be steared by designing 3D profile of nematic director. Alternatively, orientation can be controlled by imposing flow profile.

--> full backflow coupling between Q and u.

Active liquid crystal colloids

Mechanisms for stearing material flow via backflow coupling:

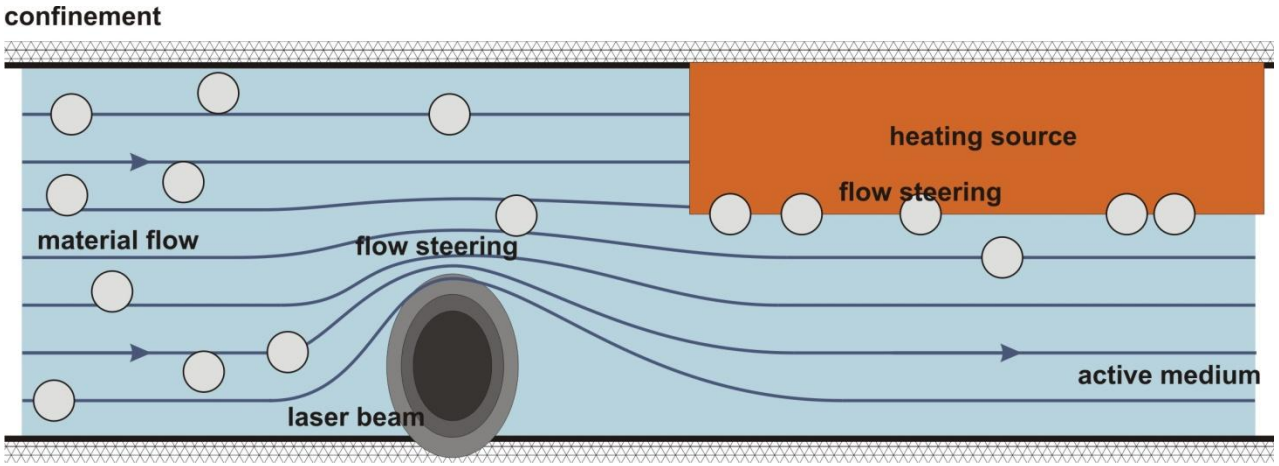

In-situ assembly of microfluidic elements:

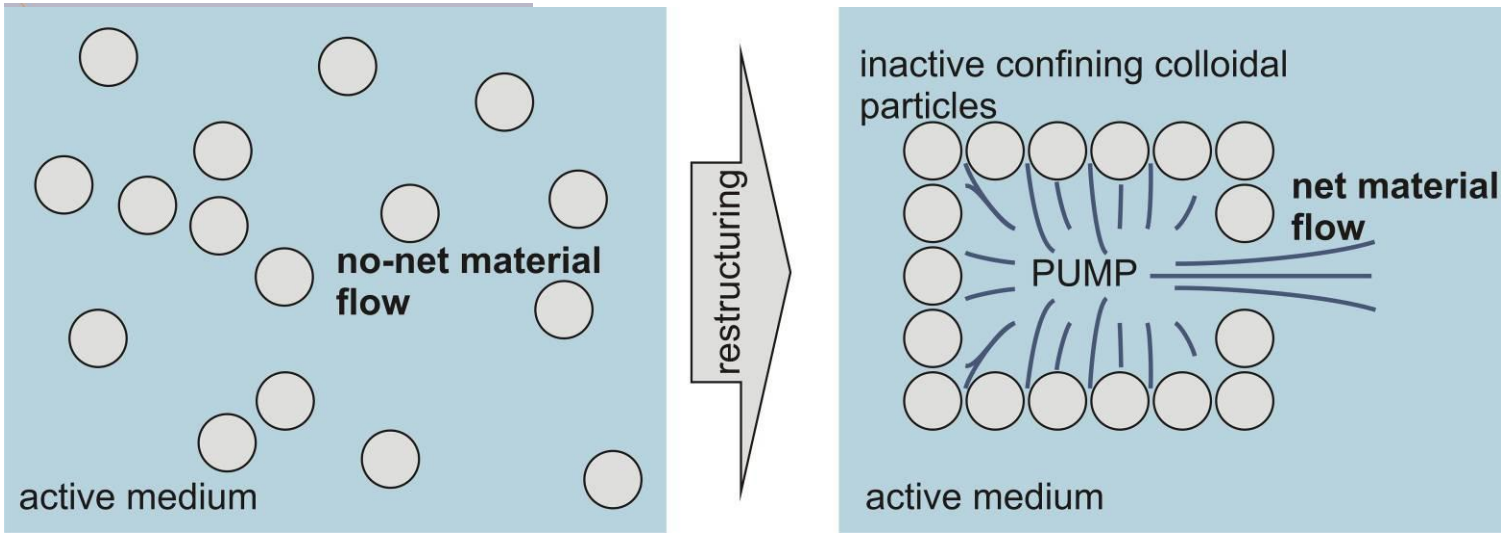

Conclusions

Functionalization of particles: shape, surface anchoring, surface profile, topological charge

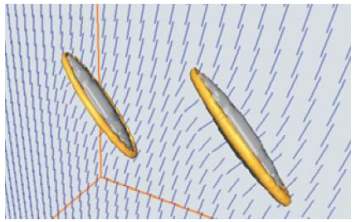

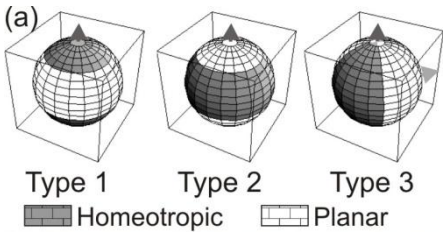

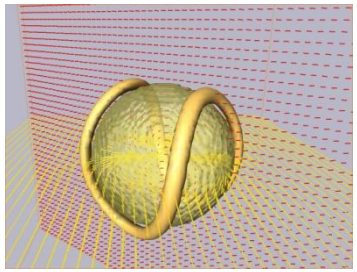

Functionalization of bulk: activity, flow stearing, confinement, colloids

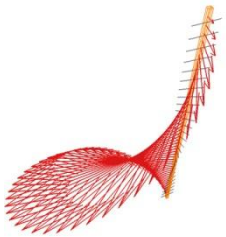

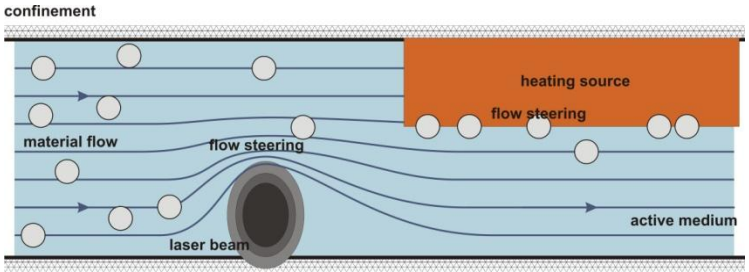

Future work: dynamics and photonics of colloidal structures, active materials.